Lymanα, Lymanα coincidence detection in the photodissociation of doubly excited molecular hydrogen into two H(2p) atoms

S. Arai, T. Kamosaki, M. Ukai, K. Shinsaka, Y. Hatano, Y. Ito, H. Koizumi, A. Yagishita, K. Ito, and K. Tanaka

Citation: The Journal of Chemical Physics **88**, 3016 (1988); doi: 10.1063/1.453943
View online: http://dx.doi.org/10.1063/1.453943
View Table of Contents: http://scitation.aip.org/content/aip/journal/jcp/88/5?ver=pdfcov
Published by the AIP Publishing

Lyman-α, Lyman-α coincidence detection in the photodissociation of doubly excited molecular hydrogen into two H(2*p*) atoms

S. Arai,[a] T. Kamosaki, M. Ukai, K. Shinsaka, and Y. Hatano
Department of Chemistry, Tokyo Institute of Technology, Meguro-ku, Tokyo 152, Japan

Y. Ito
Department of Mechanical Engineering, Technological University of Nagaoka, Nagaoka, Niigata 940-21, Japan

H. Koizumi
Faculty of Engineering, Hokkaido University, Sapporo 060, Japan

A. Yagishita, K. Ito, and K. Tanaka
Photon Factory, National Laboratory for High Energy Physics, Oho-Machi, Tsukuba-gun, Ibaraki 305, Japan

(Received 1 June 1987; accepted 29 October 1987)

Photodissociation processes of the doubly excited states of H_2 into $H(2p) + H(2p)$ have been studied using a coincidence detection of two Lyman-α photons. Coincidence spectra have been measured in the energy region of 29.0–36.0 eV. The intensity of the observed coincidence peak corresponding to two Lyman-α photons increases with increasing energy from its threshold which is about 29 eV. The main precursor of the two $H(2p)$ atoms is assigned to the doubly excited $Q_2\ ^1\Pi_u$ state.

I. INTRODUCTION

The doubly excited hydrogen molecule H_2^{**}, which decays through autoionization and dissociation, has been studied mainly in electron impact experiments.[1–8]

In the photon impact experiments, however, there exist relatively few studies until today. Autoionization of these states was studied by observing energetic protons using resonance line radiation[9,10] and synchrotron radiation.[11] Dissociation, i.e., neutral fragmentation of doubly excited states of H_2 has been successfully studied by observing Lyman-α radiation emitted from $H(2p)$ atoms using synchrotron radiation.[12] Three thresholds have been found in the Lyman-α excitation spectrum and ascribed to the excitation to optically allowed doubly excited states of H_2.[13] Lyman-α excitation spectra in the photodissociation of H_2, HD, and D_2 have been also measured.[14] And very recently the angular distribution of Lyman-α radiation in the photodissociation of doubly excited states of H_2 has been measured.[15]

Doubly excited states of H_2 have been also studied theoretically by many authors.[16–20] The calculated potential energy curves of optically allowed doubly excited states of H_2 are shown in Fig. 1 with some potential energy curves of H_2^+ summarized by Sharp.[21] These H_2^{**} states have usually been divided into two kinds of Rydberg states, i.e., the Q_1 and the Q_2 states. The Q_1 states have the $^2\Sigma_u^+(2p\sigma_u)$ state of H_2^+ as the core orbital and dissociate into $H(1s) + H(nl)$ or $H^+ + H^-$ by direct dissociation or by crossing with the one-electron excited states at a large internuclear distance. The Q_2 states have the $^2\Pi_u(2p\pi_u)$ state of H_2^+ as the core orbital and dissociate directly into two excited H atoms. The previously observed Lyman-α photons[12–15] are emitted from $H(2p)$ atoms produced through the dissociation of both Q_1 and Q_2 states into $H(2p) + H(nl)$.

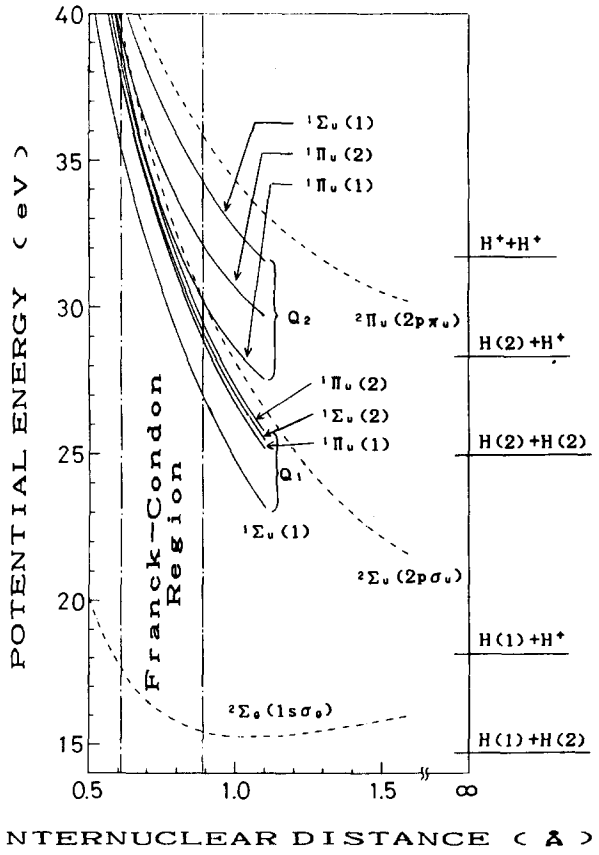

FIG. 1. Potential energy curves of doubly excited states (H_2^{**}) and ionic states (H_2^+) of H_2. H_2^{**} calculated by Takagi and Nakamura (Ref. 19) except for the $Q_2\ ^1\Sigma_u(1)$ state which was calculated by Guberman (Ref. 18). H_2^+ summarized by Sharp (Ref. 21).

[a] Present address: Central Research Laboratory, Hitachi Ltd., Kokubunji, Tokyo 185, Japan.

 0021-9606/88/053016-06$02.10

Two Lyman-α photons can be produced in the following dissociation process:

$$H_2 + h\nu \rightarrow H_2^{**} \rightarrow H(2p) + H(2p). \quad (1)$$

This process was observed for D_2 in an electron impact experiment[22] at an impact energy of 200 eV. Using synchrotron radiation, however, this process is expected to be studied in detail with a state selective excitation.

With the above mentioned background, the photodissociation of doubly excited states of H_2 into $H(2p) + H(2p)$ has been studied in this investigation by the coincidence detection of two Lyman-α photons emitted from fragment $H(2p)$ atoms using synchrotron radiation.

II. EXPERIMENTAL

A. Synchrotron radiation at the Photon Factory beam line 12 A

1. The optical system

Synchrotron radiation (SR) at the beam line 12A (BL-12A) of the Photon Factory (PF) of the National Laboratory for High Energy Physics, has been used as an excitation source. The optical system of BL-12A is schematically shown in Fig. 2. Synchrotron radiation extracted from the electron storage ring at PF was deflected by a cylindrical mirror which eliminates the short wavelength component of SR. Vertical focusing of the incident SR on the entrance slit of the monochromator was achieved with a Pt-coated concave mirror. The VUV continuum of SR was dispersed by a 1 m Seya–Namioka monochromator using a Au-coated, 2400 lines/mm grating. The monochromatized light was focused by a post-focusing mirror system, which was composed of two Au-coated plane mirrors and one Au-coated toroidal mirror and was introduced into the experimental chamber through a Au mesh which was used for a light flux monitor.

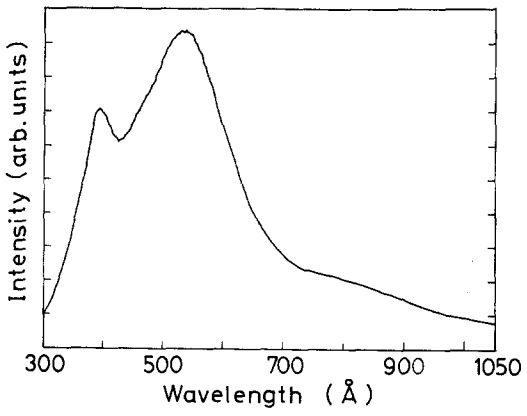

FIG. 3. Intensity spectrum of the incident SR photon flux.

2. Intensity of SR light flux

Figure 3 shows the intensity of the incident SR light flux obtained from the measurement of the absorption spectrum of Ar using an ionization chamber which was used in the measurement of the photoabsorption cross section.[23] The peak at ~400 Å is the blaze of the grating used and the peak at ~530 Å is the maximum which comes from the total reflection efficiency of the optical system at this beam line. The photon flux at the maximum was about 2×10^7 photons/mA s, when the slit width of 1.00 mm was applied in the entrance and the exit slits of the monochromator.

3. Pulse property of SR

The electron storage ring at PF has usually been operated in a multibunching mode. Its cycle is 624 ns and the interval between each bunch is 2 ns. The pulse property of SR at PF has been monitored by detecting the incident SR using a CsI-coated microchannel plate (MCP, Hamamatsu Photon-

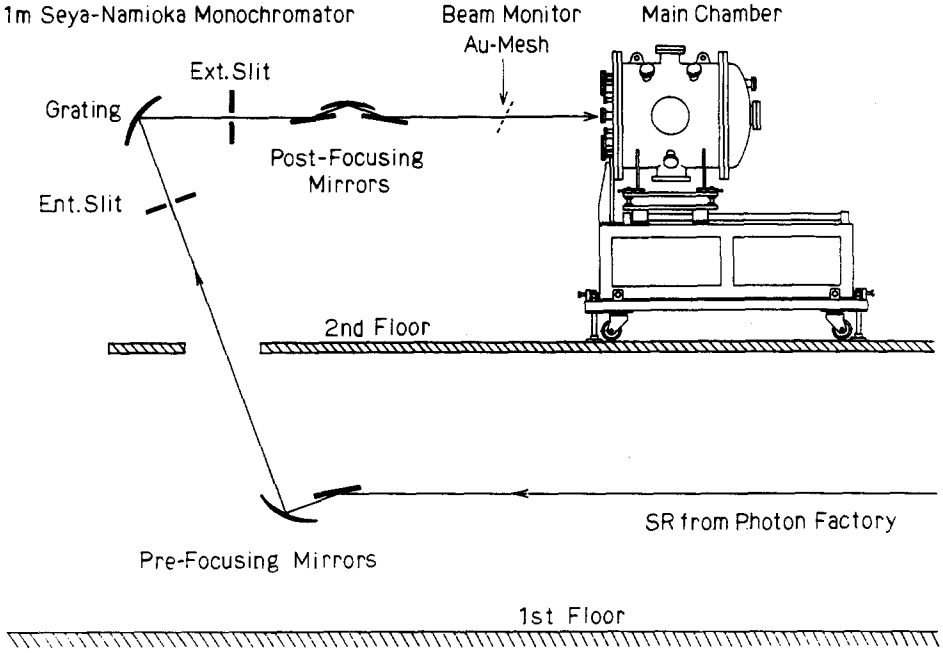

FIG. 2. Schematic view of the optical system of the BL-12A at the Photon Factory.

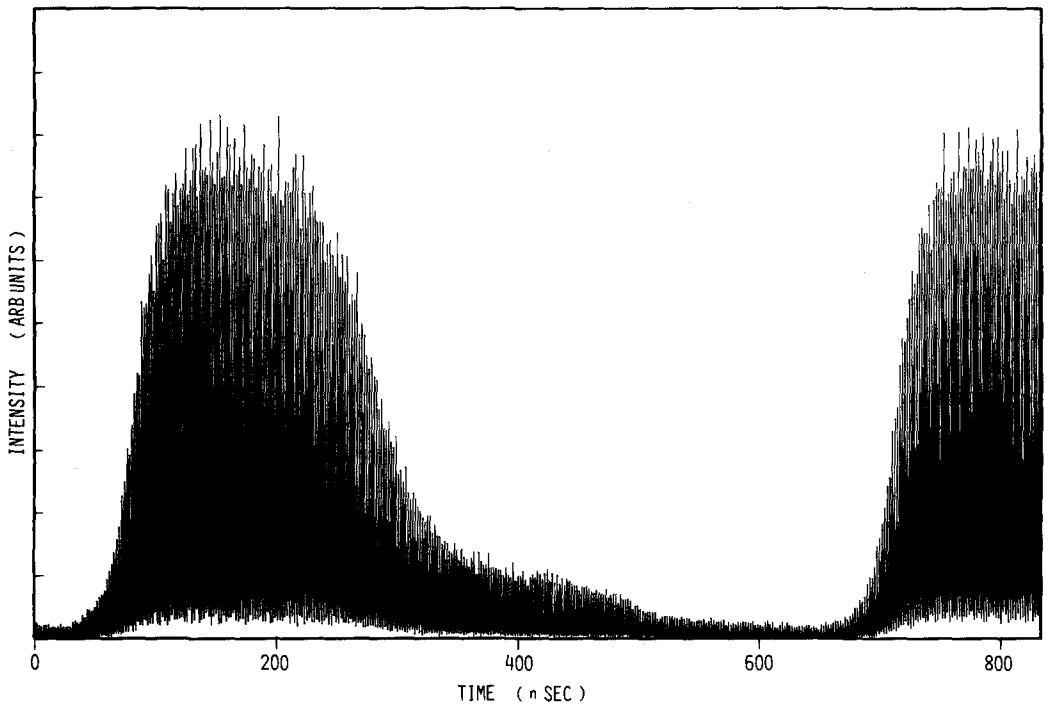

FIG. 4. Monitor of SR pulse property in a multibunching mode.

ics Co. F1094-21SX) in coincidence with the 500 MHz rf signals. The monitoring technique is almost the same as our previous ones.[24,25] An example of the whole shape of the multibunching mode is shown in Fig. 4. Electrons have not been constantly injected from the linac to prevent the ion trapping effect of electrons in the storage ring. The whole shape of the multibunching mode has varied slightly in each injection. Figure 5 shows another example of pulse monitor with higher time resolution in the same bunching mode. Each pulse of bunches has been completely resolved with FWHM of about 500 ps.

B. The setup in the experimental chamber

1. Monitor of photon flux

The monochromatized SR light beam through a Au mesh was introduced into a differentially pumped gas cell (Fig. 6), which was placed in the experimental chamber and was detected with a photomultiplier tube (PMT, Hamamatsu Photonics Co., R761) through a sodium–salicylate coated Pyrex glass. A SR light beam was monitored by measuring the ion current from the Au mesh and the electric current from the PMT. Both current intensities were mea-

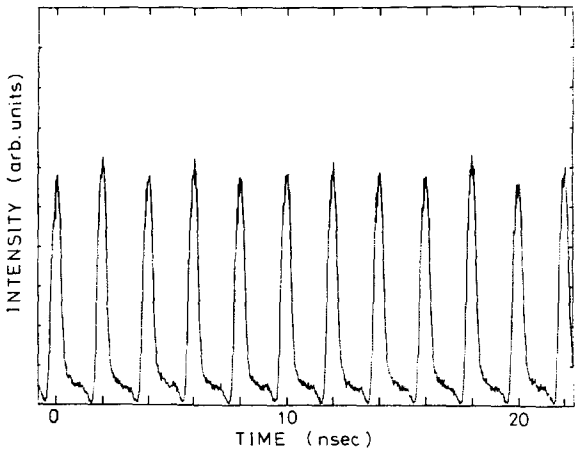

FIG. 5. Monitor of SR pulse property in a multibunching mode with higher time resolution than that of Fig. 4.

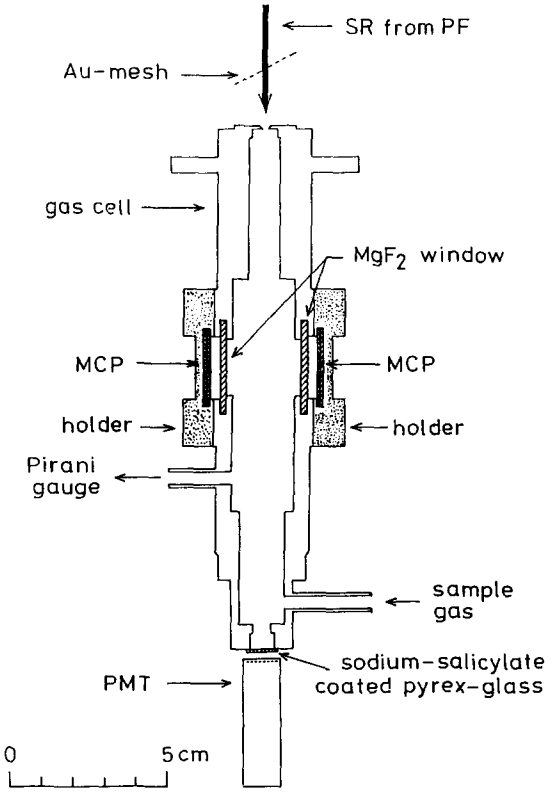

FIG. 6. Schematic view of the gas cell and Lyman-α detectors.

sured with picoammeters and through VF converters counted by counters.

2. Vacuum system and sample gas pressure

The experimental chamber was evacuated by a 1500 *l*/s turbomolecular pump (Sargent Welch Scientific Co. 3133C). The sample gas pressure in the gas cell was monitored by a Pirani gauge calibrated with an MKS capacitance manometer (Baratron). The background pressure of the chamber was monitored by an ionization gauge at the chamber wall. A background pressure of 2×10^{-7} Torr has been achieved. The sample gas pressure has been maintained to be about 2×10^{-2} Torr at the gas cell and about 4×10^{-5} Torr at the chamber wall. The gas pressure monitored at the gas cell is proportional to that at the chamber wall in this pressure region.

3. Detection of Lyman-α radiation

Lyman-α radiation produced in the gas cell was detected by two CsI-coated MCPs combined with MgF_2 windows through two apertures whose diameters are 20 mm (Fig. 6). These detectors were aligned to the direction of the main polarization plane of the linearly polarized incident SR light beam. The detection efficiency of a MCP has been much improved by coating with CsI. Compared to the detection efficiency at 1216 Å, these detection systems have effective sensitivities in the wavelength region of 1150–2000 Å.[26] Except for Lyman-α radiation, no other radiation whose wavelength is in this wavelength region can be produced in the photon impact excitation of H_2 in the impact energy region of this experiment. So the present detection system has worked as a system with considerably high signal-to-noise ratio.

C. Coincidence detection of two Lyman-α photons and data analysis

The coincidence circuit is schematically shown in Fig. 7. The output signals of one MCP were amplified and shaped by a fast preamplifier and a constant fraction discriminator (CFD) and introduced to the start input of a time-to-amplitude converter (TAC). The output signals of the other MCP were amplified and shaped similarly, and introduced to the stop input of the TAC through a delay cable. The output signals of the TAC, whose pulse heights are proportional to the interval between the times when a start and a stop signal are introduced to the TAC, were accumulated in a pulse height analyzer (PHA) which was connected to a microcomputer. And the output pulses of each CFD were counted by counters.

The relative cross section for the dissociation of H_2^{**} into $H(2p)+H(2p)$ has been obtained in the following way. Let the number of Lyman-α photons passing through the aperture of the detector in unit time be N, then N is expressed as

$$N=\sigma\cdot n_{ph}\cdot n_g\cdot\int\Delta\Omega dl, \tag{2}$$

where σ is the total cross section for producing $H(2p)$ atoms,[13] n_{ph} is the number of incident SR photons in the unit

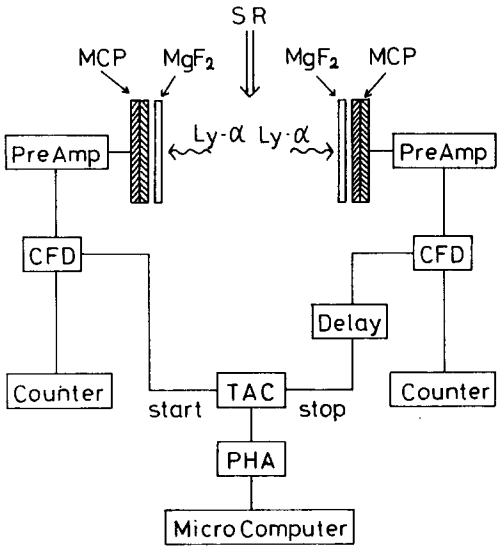

FIG. 7. Block diagram of the electric circuit for Lyman-α, Lyman-α coincidence detection.

time, n_g is the number of H_2 molecules in the unit volume, $\Delta\Omega$ is the solid angle subtended by the detector at a point on the incident light beam, and l is the path length of the light crossing the interaction region. The integration is along the incident SR beam and is constant during measurement. The values of n_{ph} and n_g are proportional to the ion current (I) from the Au mesh and the gas pressure (P) in the gas cell, respectively. Then N can be expressed by the experimentally obtained values using a proportional constant of k as

$$N=k\cdot I\cdot P\cdot\sigma. \tag{3}$$

The count rates of start and stop signals have been counted by counters and expressed by N as

$$C_a=f_a\cdot N=f_a\cdot k\cdot\sigma\cdot I\cdot P \tag{4}$$

and

$$C_b=f_b\cdot N=f_b\cdot k\cdot\sigma\cdot I\cdot P, \tag{5}$$

respectively, where f_a and f_b are constants involving the detection efficiency of each MCP and the rate of signals which can pass the discriminator of each CFD. Let the fraction of Lyman-α photons produced through the process (1) be f_c, then the rate of true coincidence C_c is expressed as

$$C_c=N\cdot f_a\cdot f_b\cdot f_c^2. \tag{6}$$

Therefore, the relation between the cross section of the process (1), σ_c, and the experimentally obtained values, i.e., σ, I, P, C_a, C_b, and C_c is expressed using Eqs. (2)–(6) as follows:

$$\begin{aligned}\sigma_c&=f_c\cdot\sigma\\&=\sqrt{\sigma^2\cdot C_c/N\cdot f_a\cdot f_b}\\&=\sqrt{N\cdot\sigma^2\cdot C_c/C_a\cdot C_b}\\&=\sqrt{k\cdot\sigma^3\cdot I\cdot P\cdot C_c/C_a\cdot C_b}.\end{aligned} \tag{7}$$

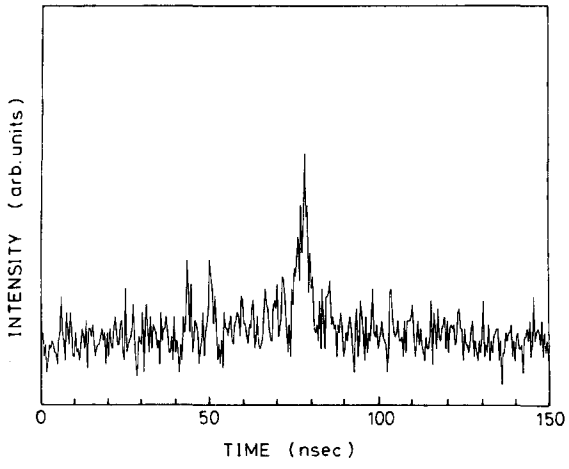

FIG. 8. Lyman-α, Lyman-α coincidence signals obtained at 33.0 eV.

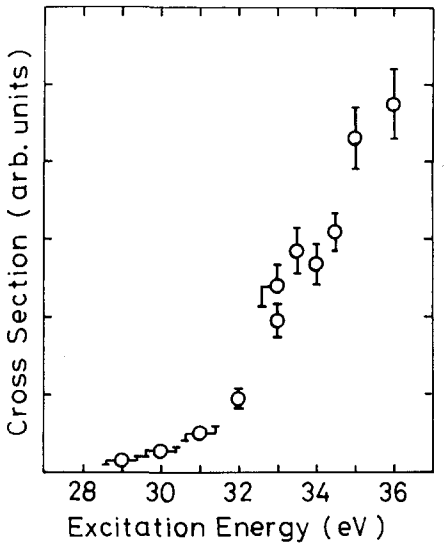

FIG. 9. Excitation spectrum of process (1) (see the text).

III. RESULTS AND DISCUSSION

An example of the obtained coincidence signals is shown in Fig. 8. A peak emerging from the background of random coincidence signals corresponds to the coincidence detection of two Lyman-α photons resulting from dissociation of doubly excited states of H_2. The peak of the true coincidence has a width of 5 ns (FWHM) and is shifted to the expected position in the time spectrum by choosing the delay time. Only background random coincidence signals have been obtained in the energy region corresponding to the excitation to one-electron excited states of H_2 which dissociate into $H(1s) + H(nl)$ $(n \geqslant 1)$.

Lyman-α radiation in the dissociation of doubly excited states of H_2 can be produced through the following processes:

$$
\begin{aligned}
H_2 + h\nu \rightarrow H_2^{**} \longrightarrow\ & H(2p) + H(2p) \\
& \downarrow \quad\ \downarrow \qquad (8)\\
& \text{Ly-}\alpha \quad \text{Ly-}\alpha, \\
\longrightarrow\ & H(2p) + H(3l) \\
& \downarrow \quad\ \downarrow \\
& \text{Ly-}\alpha \quad H(2p) \qquad (9)\\
& \qquad\quad \downarrow \\
& \qquad\quad \text{Ly-}\alpha, \\
\longrightarrow\ & H(3l) + H(3l) \\
& \downarrow \quad\ \downarrow \\
& H(2p) + H(2p) \qquad (10)\\
& \downarrow \quad\ \downarrow \\
& \text{Ly-}\alpha \quad \text{Ly-}\alpha, \\
\longrightarrow\ & H(2s) + H(2p) \\
& \qquad\quad \downarrow \qquad (11)\\
& \qquad\quad \text{Ly-}\alpha, \\
\longrightarrow\ & H(2s) + H(3l) \\
& \qquad\quad \downarrow \\
& \qquad\quad H(2p) \qquad (12)\\
& \qquad\quad \downarrow \\
& \qquad\quad \text{Ly-}\alpha.
\end{aligned}
$$

Two Lyman-α photons produced through the process (8), (9), or (10) have a time correlation between the two and can be detected as a true coincidence signal. Lyman-α photons produced through processes (11) and (12) cause background random coincidence signals. Since all the Lyman-α photons produced through processes (8)–(12) cannot be detected because of the loss factor of the detector, i.e., quantum efficiencies of detectors and the angular distributions of Lyman-α photons, then Lyman-α photons produced through processes (8)–(10) can also cause the random coincidence signals.

As the lifetime of $H(2p)$ state is 1.6 ns, Lyman-α photons produced through the process (8) cause the sharp true coincidence peak as observed in this experiment. The lifetimes of $H(3s)$, $H(3p)$, and $H(3d)$ are 160, 5.4, and 15.6 ns, respectively,[27] so Lyman-α photons produced through cascades produce a broader component in the true coincidence peak. Such a broad component in the peak of true coincidence, however, cannot be found in Fig. 8. Although the intensity of the incident SR photon flux decreases monotonically with decreasing electric current of electrons in the storage ring in a macroscopic time scale, it varies periodically in a microscopic time scale (Fig. 5). Hence the background random coincidence spectrum is not so flat, which makes it difficult to find the broad component in the coincidence signal. The production cross section of $H(nl)$ decreases much with increasing n,[28] so Lyman-α photons produced through cascades cannot have a large contribution to the peak of true coincidence.

It is, therefore, concluded that the coincidence peak almost at the center of the coincidence signals in Fig. 8 is assigned to process (8).

Subtracting the background random coincidences, the relative cross section of process (1) [i.e., process (8)] has been obtained using Eq. (7) and shown in Fig. 9. The cross section has the threshold at the energy just below 29 eV and increases with increasing energy. The experimental errors are about $\pm$ 10% of the cross section values. Their absolute

errors, however, increase by increasing the energy because of the decrease in the intensity of the incident SR flux. The observed threshold in Fig. 9 is clearly larger than the first threshold (26.6 eV) in the Lyman-α excitation spectrum[13] and is close to the second (29.2 eV) and the third (30.9 eV) thresholds.

The precursor of the observed two $H(2p)$ atoms in the process (1) is H_2^{**} in the doubly excited Q_2 state, which dissociate into two excited H atoms. The Q_1 states dissociate into $H(1s) + H(nl)$ and cannot be the precursor of the observed two $H(2p)$ atoms. The $Q_2\ ^1\Pi_u(1)$ state must be the precursor of process (1) because it is the lowest Q_2 state and is expected to dissociate into the lowest limit of the Q_2 state, i.e., $H(2p) + H(2p)$ at 24.9 eV. The experimentally obtained threshold (about 29 eV) of process (1) is smaller than, as shown in Fig. 1, the threshold energy (about 30 eV) as expected from the calculated potential curves of the $Q_2\ ^1\Pi_u(1)$ state in the Franck–Condon region. The reason for this discrepancy might be ascribed to either the fact that the excitation to the doubly excited states occurs slightly outside the Franck–Condon region (Fig. 1), or to some uncertainty in the theoretical potential curves.

ACKNOWLEDGMENTS

The authors wish to thank the members at the Photon Factory of the National Laboratory for High Energy Physics for supporting the present research.

[1]F. J. de Heer, H. R. Moustafa Moussa, and M. Inokuti, Chem. Phys. Lett. **1**, 484 (1967).
[2]M. Misakian and J. C. Zorn, Phys. Rev. A **6**, 2180 (1972).
[3]A. Crowe and J. W. McConkey, Phys. Rev. Lett. **31**, 192 (1973).
[4]J. A. Schiavone, K. C. Smyth, and R. S. Freund, J. Chem. Phys. **63**, 1043 (1975).
[5]K. Ito, N. Oda, Y. Hatano, and T. Tsuboi, Chem. Phys. **17**, 35 (1976).
[6]C. Karolis and E. Harting, J. Phys. B **11**, 357 (1978).
[7]K. Köllmann, J. Phys. B **11**, 331 (1978).
[8]Y. Hatano, Comments At. Mol. Phys. **13**, 259 (1983), and references cited therein.
[9]S. Strathdee and R. Browning, J. Phys. **9**, L505 (1976).
[10]S. Strathdee and R. Browning, J. Phys. **12**, 1789 (1979).
[11]T. Masuoka, J. Chem. Phys. **81**, 2652 (1984).
[12]S. Arai, T. Yoshimi, H. Koizumi, K. Shinsaka, K. Hironaka, M. Morita, T. Yoshida, A. Yagishita, K. Ito, and Y. Hatano, Proceedings of 14th International Conference on the Physics of Electronic and Atomic Collisions, Stanford (1985), p. 55.
[13]S. Arai, T. Yoshimi, M. Morita, K. Hironaka, T. Yoshida, H. Koizumi, K. Shinsaka, Y. Hatano, A. Yagishita, and K. Ito, Z. Phys. D **4**, 65 (1986).
[14]M. Glass-Maujean, J. Chem. Phys. **85**, 4830 (1986).
[15]S. Arai, K. Shinsaka, T. Kamosaki, M. Ukai, Y. Ito, H. Koizumi, A. Yagishita, K. Tanaka, and Y. Hatano, Proceedings of 15th International Conference on the Physics of Electronic and Atomic Collisions, Brighton (1987).
[16]C. Bottcher, J. Phys. B **7**, L352 (1974).
[17]A. U. Hazi, J. Phys. B **8**, L262 (1975).
[18]S. L. Guberman, J. Chem. Phys. **78**, 1404 (1983).
[19]H. Takagi and H. Nakamura, Phys. Rev. A **27**, 691 (1973).
[20]J. Tennyson, C. J. Noble, and S. Salvini, J. Phys. B **17**, 905 (1984).
[21]T. E. Sharp, At. Data **2**, 119 (1971).
[22]N. Böse, J. Phys. B **11**, L309 (1978).
[23]H. Koizumi, K. Hironaka, K. Shinsaka, S. Arai, H. Nakazawa, A. Kimura, Y. Hatano, Y. Ito, Y. Zhang, A. Yagishita, K. Ito, and K. Tanaka, J. Chem. Phys. **85**, 4276 (1986).
[24]Y. Hatano, M. Ohno, N. Kouchi, H. Koizumi, A. Yokoyama, G. Isoyama, H. Kitamura, and T. Sasaki, Chem. Phys. Lett. **84**, 454 (1981).
[25]K. Shinsaka, H. Koizumi, T. Yoshimi, N. Kouchi, Y. Nakamura, M. Toriumi, M. Morita, Y. Hatano, S. Asaoka, and H. Nishimura, J. Chem. Phys. **83**, 4405 (1985).
[26]C. Martin and S. Bowyer, Appl. Opt. **21**, 4206 (1982).
[27]H. Bethe and E. E. Salpeter, in *Handbuch der Physik*, edited by S. Flugge (Springer, Berlin, 1957), Vol. 35, p. 355.
[28]D. A. Vroom and F. J. de Heer, J. Chem. Phys. **50**, 580 (1969).